IFSM-73-46

INSTITUTE OF FRACTURE AND SOLID MECHANICS

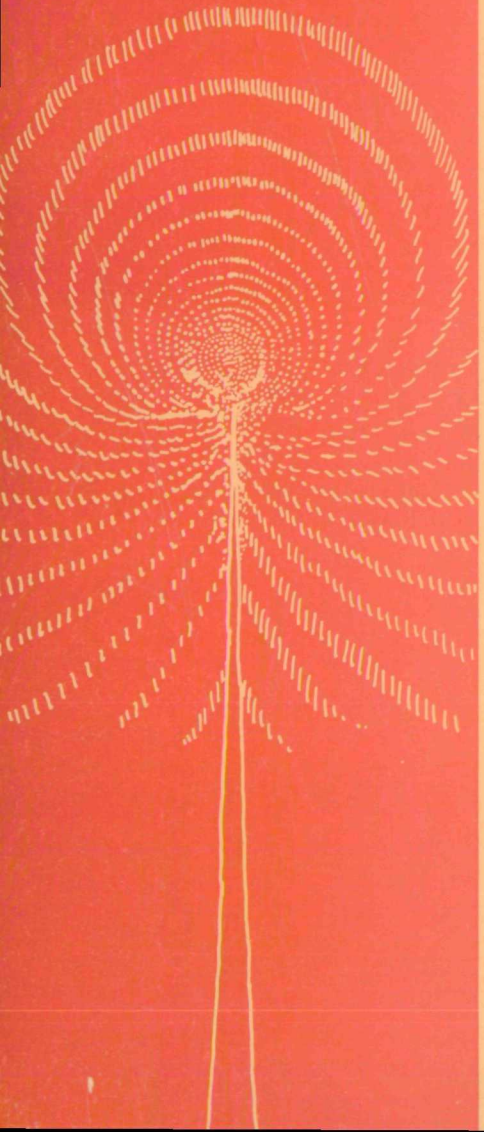

# LEHIGH UNIVERSITY

## GROWTH CHARACTERISTICS OF A PLANE CRACK SUBJECTED TO THREE-DIMENSIONAL LOADING

BY

R. J. HARTRANFT

AND

G. C. SIH



TECHNICAL REPORT NASA-TR-73-4

JULY 1973

NATIONAL AERONAUTICS AND SPACE ADMINISTRATION

LANGLEY RESEARCH CENTER

HAMPTON, VIRGINIA 23365

NATIONAL AERONAUTICS AND SPACE ADMINISTRATION

Grant NGR-39-007-066

Technical Report No. 4

# GROWTH CHARACTERISTICS OF A PLANE CRACK SUBJECTED TO THREE-DIMENSIONAL LOADING

by

R. J. Hartranft
Associate Professor of Mechanics

and

G. C. Sih
Professor of Mechanics and Director,
Institute of Fracture and Solid Mechanics

Institute of Fracture and Solid Mechanics
Lehigh University
Bethlehem, Pennsylvania 18015

July 1973

ABSTRACT

The closed form expressions for the stress intensity factors due to concentrated forces applied to the surfaces of a half plane crack in an infinite body are used to generate solutions for distributed loads in this geometry. The stress intensity factors for uniformly distributed loads applied over a rectangular portion of the crack surface are given in closed form. An example of non-uniformly distributed loads which can be treated numerically is also included. In particular, combinations of normal and shear stresses on the crack which simulate the case of loading at an angle to the crack front are considered. The resulting stress intensity factors are combined with the strain energy density fracture criterion for the purpose of predicting the most likely direction of crack propagation. The critical value, $S_c$, of the energy density factor can then be used for determining the allowable load on a specimen with a crack front not perpendicular to the tensile axis.

## INTRODUCTION

As one of the most common types of flaws, the surface crack has generated a good deal of interest [1]. The extreme difficulty of treating numerically the region of intersection of the crack front with a free surface has been demonstrated in [2]. Additional, more fundamental, research is indicated for three-dimensional crack problems so that a better understanding of the nature of their exact elasticity solutions can be obtained. This paper considers some problems which can be solved exactly and which may contribute to this understanding.

The basic geometry considered is identical to that of the plane strain semi-infinite crack problem. In three-dimensions it is described as a half plane crack in an infinite material. The body is continuous except for a discontinuity along the entire half of the xz-plane for which $x<0$. A three-dimensional view of the geometry is given in Figure 1. There are two sources for the stress intensity factors due to concentrated forces on the crack. The solution for the components P and Q parallel to the y- and x-axes, respectively (on the upper crack surface; on the lower surface the directions are opposite those on the upper surface) has been obtained in [3] from the solution in [4]. The solution for the remaining component, R, parallel to the z-axis has been given in [5]. The expressions will be given in the next section.

As will be seen by examining the solutions, unless the loads on the crack are normal to the surfaces, there will be a mixture of the three basic modes of crack deformation. In this case, the energy release rate approach of the classical theory of fracture mechanics is no longer applicable since it is for a crack propagating in a self-similar manner. In order to apply the results for the stress intensity factors, a fracture criterion proposed in [6], which uses the crack front strain energy density field, will be used. This criterion predicts that crack growth will occur in the direction of minimum strain energy density at a load which produces a certain critical value of the strain energy density along this direction. Under predominantly mode I loading, the energy density associated with volume change along this direction is found to be greater than that of distortion or change in shape.

The results are qualitatively similar to some which have been obtained experimentally for a nearly longitudinal shear loading [7]. That is, they predict that the surface of crack extension makes an angle with the initial crack front. In two-dimensional plane problems, the new crack surface always contains the initial crack front.

Caution should be used in making physical predictions based on these results. The energy density criterion gives the expected fracture direction for the current geometry. Once the crack begins to extend from the most highly stressed segment of the crack front zone, the geometry, and hence the

entire solution, is altered. In a recent dissertation [8], however, there are results which show that for some materials, the solution based on initial geometry can be used after crack extension has significantly changed the geometry. Therefore, it does not seem unlikely that the present results will hold for some materials and give an explanation for the tilting of the crack growth relative to the initial crack front.

## STRAIN ENERGY DENSITY THEORY

The strain energy density in the neighborhood of the crack front is given by

$$\frac{dW}{dV} = \frac{S}{\rho} \tag{1}$$

where $\rho$ is the distance from the z-axis, the crack front. The factor S represents the intensity of the energy density field, dW/dV. Because of geometric and material uncertainties in real situations, equation (1) is used only outside of a core region having a finite radius $\rho = \rho_o(z)$ as shown in Figure 1. The actual size of this region depends on the crack tip radius and will not be elaborated on here since the present analysis assumes a sharp crack.

The factor S, appearing in equation (1), which is used in the fracture criterion is related to the stress intensity factors by

$$S = a_{11}k_1^2 + 2a_{12}k_1k_2 + a_{22}k_2^2 + a_{33}k_3^2 \tag{2}$$

The coefficients in equation (2) are dependent on the shear modulus, $\mu$, Poisson's ratio, $\nu$, and the angle $\theta$ of the usual cylindrical coordinates $(\rho,\theta,z)$ through

$$16\mu a_{11} = (1+\cos\theta)(3-4\nu-\cos\theta)$$

$$16\mu a_{12} = -2\sin\theta(1-2\nu-\cos\theta) \tag{3}$$

$$16\mu a_{22} = 4(1-\nu)(1-\cos\theta) - (1+\cos\theta)(1-3\cos\theta)$$

$$16\mu a_{33} = 4$$

The fracture criterion based on the strain energy density concept may be stated as follows [6]:

(1) The crack grows in a direction for which S reaches a minimum, i.e.,

$$\frac{\partial S}{\partial \theta} = 0, \quad \frac{\partial^2 S}{\partial \theta^2} > 0 \text{ at } \theta = \theta_c \tag{4}$$

where $\theta_c$ is the angle between the plane of the original crack and the segment of new crack growth.

(2) The crack growth begins when S reaches a critical value $S_c$, i.e.,

$$S(k_1,k_2,k_3) = S_c \text{ at } \theta = \theta_c \tag{5}$$

where $S_c$ is a material parameter.

Under conditions in which the opening mode of crack deformation is predominant, it is found that the portion of the minimum value of S which is associated with change of volume

is larger than the portion due to change of shape. The converse is true of the maximum values of S, which associates the maxima with the von Mises yield condition of plasticity. A detailed discussion of this can be found in [9].

CONCENTRATED LOAD ON THE CRACK

Consider an infinite body containing the half plane crack shown in Figure 1 with a concentrated force having components (Q,P,R) acting at the point $(-a,0^+,0)$ of the upper crack surface and a concentrated force (-Q,-P,-R) at point $(-a,0^-,0)$ of the lower crack surface. The stress intensity factors for the components, P and Q, are given in [3], and those for the remaining component, in [5]. They may be expressed in the form

$$k_1 = \frac{1}{\pi^2 a}\sqrt{\frac{2}{a}}\, P f_1(z/a)$$

$$k_2 = \frac{1}{\pi^2 a}\sqrt{\frac{2}{a}}\left\{Q f_1(z/a) + \frac{2\nu}{2-\nu}\left[Q f_2(z/a) + R f_3(z/a)\right]\right\} \quad (6)$$

$$k_3 = \frac{1}{\pi^2 a}\sqrt{\frac{2}{a}}\left\{R f_1(z/a) + \frac{2\nu}{2-\nu}\left[R f_2(z/a) + Q f_3(z/a)\right]\right\}$$

where the functions which describe the variation of the stress intensity factors along the crack front are given by

$$f_1(\zeta) = \frac{1}{1+\zeta^2}$$

$$f_2(\zeta) = \frac{1-\zeta^2}{(1+\zeta^2)^2} \quad (7)$$

$$f_3(\zeta) = \frac{2\zeta}{(1+\zeta^2)^2}$$

For the case when the forces are applied to the points $(-a,0^{\pm},z_o)$ instead of $(-a,0^{\pm},0)$, one need only replace z by

$z-z_o$ in equations (6).

In order to simulate the case of stresses acting at an angle $\beta$ to the crack front, the relations

$$P = \frac{1}{2} F(1+\cos 2\beta)$$

$$Q = 0 \qquad (8)$$

$$R = -\frac{1}{2} F \sin 2\beta$$

will be used. These are the relations which give the components of stress on a plane oriented as shown in Figure 2 in a state of uniform stress. This point will be brought up again in the section on distributed loads; for now, equations (8) are a way of expressing the forces in terms of a single parameter, F, which can be interpreted as the product of the stress vector on the surface and a small element of area of the surface.

It is a straightforward calculation, given $\beta$, to substitute from equations (8) into (6) into (2), and then to locate the angle $\theta_c$ for which S is a minimum. The result of this calculation is shown in Figure 3 for $\beta = 45°$ (P=-R, Q=0) and $\nu$=0.30. The angle, $\theta_c$, which gives the direction of expected crack propagation increases as points further out along the z-axis are considered until, ultimately, the effect of the force disappears, and the crack does not extend. For negative values of z, the behavior is the same except that the angle,

$\theta_c$, is negative. The sketch in Figure 4 shows the directions of the forces, P and R, and the expected direction of crack growth at each point of the crack front.

Crack growth begins at z=0, for the minimum value of S at that point reaches $S_c$ first as the forces are increased. The first growth alters the geometry and casts doubt on further application of this analysis. However, the work reported in [8] on two-dimensional theory and experiment shows that the predictions based on initial geometry may be used, at least for the materials tested, well after the geometry has been altered. Thus, the directions of growth indicated in Figures 3 and 4 may be accepted with caution until growth has proceeded quite far. Since the central portion of the crack begins to run first, it would be expected to grow more than other portions. Thus, Figure 4 could be made to represent the new crack front shape if the lines showing the direction of crack growth were made to decrease in length as z increases in magnitude. This gives a qualitative description of new crack surface similar to that observed in [7].

## DISTRIBUTED STRESSES ON THE CRACK

The solutions given by equations (6) and (7) of the previous section may be used as Green's functions to generate stress intensity factors for arbitrary distributions of stress on the crack surfaces. The formulation of general equations involving double integrals proceeds in the usual way. Of interest here is the case where the stresses on the surfaces of the crack are given by constants,

$$\sigma_y = -p, \quad \tau_{xy} = -q, \quad \tau_{yz} = -r \tag{9}$$

on the rectangular region $-b \leq x \leq 0$, $-a \leq z \leq a$ shown on Figure 5 and are zero everywhere else. In this case the integrals may be evaluated in closed form, and the results can also be used to generate numerical solutions for the case of variable applied stresses. Limiting special cases are presented in the Appendix.

After performing the required integrations, the solution for the case of stresses applied uniformly to a rectangular portion of the crack surfaces may be written as

$$\begin{aligned} k_1 &= \frac{1}{\pi^2} pF_1 \\ k_2 &= \frac{1}{\pi^2} \{qF_1 + \frac{2\nu}{2-\nu} [qF_2 - rF_3]\} \\ k_3 &= \frac{1}{\pi^2} \{rF_1 + \frac{2\nu}{2-\nu} [rF_2 - qF_3]\} \end{aligned} \tag{10}$$

where $F_1$, $F_2$, $F_3$ depend on z,a,b through

$$F_1 = \sqrt{|z|+a}\; g_1\left(\frac{b}{|z|+a}\right) - \mathrm{sgn}(|z|-a)\sqrt{||z|-a|}\; g_1\left(\frac{b}{||z|-a|}\right)$$

$$F_2 = \sqrt{|z|+a}\; g_2\left(\frac{b}{|z|+a}\right) - \mathrm{sgn}(|z|-a)\sqrt{||z|-a|}\; g_2\left(\frac{b}{||z|-a|}\right)$$

$$F_3 = \mathrm{sgn}(z)\left[\sqrt{|z|+a}\; g_3\left(\frac{b}{|z|+a}\right) - \sqrt{||z|-a|}\; g_3\left(\frac{b}{||z|-a|}\right)\right] \tag{11}$$

in which the functions $g_1$, $g_2$, $g_3$ are given by

$$g_1(\eta) = 2\sqrt{2\eta}\,\arctan\frac{1}{\eta} + \log\frac{1+\eta-\sqrt{2\eta}}{1+\eta+\sqrt{2\eta}} + 2\arctan(\sqrt{2\eta}+1) + 2\arctan(\sqrt{2\eta}-1)$$

$$g_2(\eta) = \frac{1}{2}\log\frac{1+\eta-\sqrt{2\eta}}{1+\eta+\sqrt{2\eta}} + \arctan(\sqrt{2\eta}+1) + \arctan(\sqrt{2\eta}-1) \tag{12}$$

$$g_3(\eta) = 2\sqrt{2\eta} + \frac{1}{2}\log\frac{1+\eta-\sqrt{2\eta}}{1+\eta+\sqrt{2\eta}} - \arctan(\sqrt{2\eta}+1) - \arctan(\sqrt{2\eta}-1)$$

and the signum function, sgn(z), is +1, 0, or -1 depending on whether the argument, z, is positive, zero, or negative, respectively.

By such standard techniques as superposition and change of coordinates, equations (10) to (12) can be used to obtain the stress intensity factors due to uniform stresses on an arbitrary rectangular portion of the crack surfaces. For a rectangle of sides c and d in the z- and x-directions, respec-

tively, which is centered about the point $(-x_o, 0, z_o)$, all that is required is to replace

$$F_i(z,a,b), \quad i = 1,2,3$$

of equations (10) by

$$F_i(z-z_o, \frac{c}{2}, x_o + \frac{d}{2}) - F_i(z-z_o, \frac{c}{2}, x_o - \frac{d}{2}), \quad i = 1,2,3$$

where it should be noted that $x_o \geq d/2$, and that for $x_o = d/2$, the second term vanishes.

An arbitrary distribution of stress on the crack surfaces may be approximated by piecewise constant stresses, and the above solution applied for each rectangular subportion of the surfaces. This technique will be applied in a numerical example in the next section.

## FRACTURE ANGLE FOR DISTRIBUTED STRESSES

The solution given by equations (10) - (12) in the previous section may be used to generate solutions for arbitrary distributions of stress on the crack surfaces. Return again to the uniform stress state illustrated in Figure 2. The standard procedure for solving a crack problem is to compute the stress at the location of the crack (the xz-plane) in an uncracked body, and to apply the opposite of these stresses to the crack in an otherwise unloaded body. In this case the stresses on the xz-plane are

$$\sigma_y = p = \frac{1}{2}\sigma\,(1+\cos 2\beta)$$

$$\tau_{yz} = r = -\frac{1}{2}\sigma \sin 2\beta \qquad (13)$$

$$\tau_{yx} = q = 0$$

and, to solve the crack problem, one must apply the opposite stresses,

$$\sigma_y = -p \quad \tau_{yz} = -r, \; \tau_{yx} = -q = 0 \qquad (14)$$

to the crack surfaces.

Equations (10) - (12) may be applied directly in the case for which

$$\sigma(x,z) = \begin{cases} \sigma_o, \text{ for } -b \leq x \leq 0 \text{ and } -a \leq z \leq a \\ \\ 0 \text{ , otherwise} \end{cases} \qquad (15)$$

The parameters given by equations (13) and (15) then determine the stress intensity factors for various values of $\beta$, b/a, and $\nu$. Once the stress intensity factors are known, the location of the minimum value of the strain energy density can be found as before. Figures 5 and 6 show the variation of the direction of crack growth for $\nu = 0.3$, b/a = 0.5 and 2.0, and several values of $\beta$. For negative z, the angle, $\theta_c$, is negative with the same variation in magnitude. The crack is thus expected to run nearly straight ahead near the center of the rectangular area, but then to tilt near the ends so that the crack tends to grow toward a state in which its new crack growth plane is closer to perpendicular to the applied stress vector. Increasing $\beta$, the angle of loading, increases the tilting of the new surface. Figure 7 shows more clearly the effect of changing the area of load application. For $\nu = 0.3$ and $\beta = 30°$, increasing b/a (i.e., increasing the three-dimensional character of the problem) increases the crack angle $\theta_c$ within the loaded segment of the crack front. On the remainder of the crack front the larger values of b/a seem to stretch out the curves to peak later and decay more slowly after peaking. Decreasing b/a (which may be considered effected by increasing a toward the two-dimensional case) gives a pronounced peak at z=a, the end of the loaded portion of the crack front.

Except in the neighborhood of this point, the angle $\theta_c$ decreases to zero as b/a decreases.

As a second illustration, the same rectangular area of application of stress is used, but the stress varies over the area and becomes zero on three sides. The form used is

$$\sigma = \begin{cases} \sigma_m(1 + \frac{x}{b})(1 - \frac{z^2}{a^2}), & -b \leq x \leq 0 \text{ and } -a \leq z \leq a \\ 0, & \text{otherwise} \end{cases} \tag{16}$$

The calculations described previously are repeated for the same parameters ($\nu = 0.30$, $b/a = 0.5, 2.0$, $\beta = 10°, 30°, 50°$) with the results shown in Figures 8 and 9. The physical interpretation is the same as before, but it may be noted that the tilting of the crack plane begins earlier.

## FRACTURE LOADS FOR DISTRIBUTED STRESS

The most severely loaded portion of the crack front is at the midpoint of the loaded region. Expressions (11) simplify considerably for z=0 to give the strain energy density at that point as

$$S = \frac{a}{\pi^4 \mu} \sigma^2 \{(1-2\nu)(p/\sigma)^2 [g_1(b/a)]^2 + (r/\sigma)^2 [g_1(b/a) + \frac{2\nu}{2-\nu} g_2(b/a)]^2\} \quad (17)$$

As $a \to \infty$, the two-dimensional result

$$S = \frac{2b}{\pi^2 \mu} \sigma^2 \{(1-2\nu)(p/\sigma)^2 + (r/\sigma)^2\} \quad (18)$$

is recovered.

The criterion of fracture, equation (5) gives the fracture stress in terms of the critical value, $S_c$, of the strain energy density factor. The two-dimensional result is

$$\sigma_o = \pi \sqrt{\mu S_c / 2b} \{(1-2\nu)(p/\sigma)^2 + (r/\sigma)^2\}^{-1/2} \quad (19)$$

and the three-dimensional one,

$$\sigma_c = \pi^2 \sqrt{\mu S_c / a} \{(1-2\nu)(p/\sigma)^2 [g_1(b/a)]^2 + (r/\sigma)^2 [g_1(b/a) + \frac{2\nu}{2-\nu} g_2(b/a)]^2\}^{-1/2} \quad (20)$$

Using relations (13), the two- and three-dimensional fracture stresses may be represented as in Figure 10. This shows an initial decrease of the critical applied stress and then an unlimited increase as the angle, $\beta$, of the load is increased. The infinite fracture stress at $\beta=90^\circ$ is to be expected, for the load is then parallel to the crack surface. As the length, 2a, of the rectangular area of load application decreases, the fracture stress increases from the two-dimensional value. Again, this is expected because as the area increases, loads are being added to the surfaces of the crack. This effect is present in the two-dimensional case, and can be partly separated from the three-dimensional effects. In Figure 11, the three-dimensional fracture stresses have been normalized by the two-dimensional values. When this is done the increasing values of $\beta$ lead to steadily decreasing values of $\sigma_c/\sigma_o$, indicating greater three-dimensional effects when the load is nearly perpendicular to the crack. Figure 12 shows how little the angle $\beta$ affects the ratio of the three- to the two-dimensional fracture stress.

## CONCLUSIONS

Using either the concentrated load solution of equations (6) and (7) or the uniform load solution of equations (10), (11), and (12), it is possible to compute stress intensity factors for arbitrary distributions of stress on the faces of a half plane crack. For those cases considered in this paper, a tilting of the crack plane as the crack extends is predicted. The tilting is a change from a flat to a curved, non-cylindrical surface, which on a small scale is approximately flat and at a non-zero angle to the initial crack front. Such results appear experimentally [7] in shear loading. For purely shear loading (P=Q=0) the procedure followed here predicts no tilting. However, in the experimental set-up of [7], it is quite likely that some normal loading existed to keep the specimen from turning under application of the loads. Refer to [7] for drawings and photographs of the experiment. Thus, there is qualitative agreement of the experiment with this analysis.

REFERENCES


[1] The Surface Crack, J. L. Swedlow, ed., ASME, New York, 1972.

[2] R. J. Hartranft and G. C. Sih, "Alternating Method Applied to Edge and Surface Crack Problems", Methods of Analysis and Solutions of Crack Problems, G. C. Sih, ed., Noordhoff International Publishing, Leyden, The Netherlands, 1973, pp. 179-238.

[3] G. C. Sih and H. Liebowitz, "Mathematical Theories of Brittle Fracture", Fracture, Vol. II, H. Liebowitz, ed., Academic Press, New York, 1968, pp. 67-190.

[4] Y. S. Uflyand, "Survey of Articles on the Application of Integral Transforms in the Theory of Elasticity", University of North Carolina, Raleigh, N. C., 1965.

[5] M. K. Kassir and G. C. Sih, "Application of Papkovich-Neuber Potentials to a Crack Problem", Int. J. Sol. Struct., Vol. 9, 1973, pp. 643-654.

[6] G. C. Sih, "A Special Theory of Crack Propagation", Methods of Analysis and Solutions of Crack Problems, G. C. Sih, ed., Noordhoff International Publishing, Leyden, The Netherlands, 1973, pp. XXI-XLV.

[7] W. G. Knauss, "An Observation of Crack Propagation in Anti-Plane Shear", Int. J. Fract. Mech., Vol. 6, 1970, pp. 183-187.

[8] M. E. Kipp, Fracture of Notched Elastic Solids, Ph.D. Dissertation, Lehigh University, 1973.

[9] G. C. Sih, "Handbook of Stress-Intensity Factors", Vol. I, Institute of Fracture and Solid Mechanics Publication, Lehigh University, 1973.

## APPENDIX: SPECIAL CASES

The basic solution is given by equations (10), (11), and (12) for a uniform distribution of equal and opposite stresses applied to a rectangular area of the crack surfaces.

Line load parallel to z-axis. By superposition, the solution for uniform stresses on a rectangle bounded by $z = \pm a$, $x = -b$, $x = -c$ $(c>b)$ is obtained. If then the limit $c \to b$ is taken while holding the total load, 2aP, 2aQ, 2aR, constant, the solution for a load uniformly distributed along the line $y=0$, $x = -b$, $|z| \leq a$ is obtained. The stress intensity factors are given by equations (10) and (11) (with p,q,r replaced by P,Q,R) except that in place of $g_1$, $g_2$, $g_3$ as given by equations (12), the derivatives

$$g_1'(\eta) = \sqrt{\frac{2}{\eta}} \arctan\left(\frac{1}{\eta}\right)$$

$$g_2'(\eta) = \frac{\sqrt{2\eta}}{1+\eta^2} \qquad (21)$$

$$g_3'(\eta) = \frac{\eta\sqrt{2\eta}}{1+\eta^2}$$

are used.

Line load along x-axis. If the side of the rectangle of length 2a is shrunk to zero while the total load, bP, bQ, bR, is held constant, the case of a line load on the segment (-a,o) of the x-axis is obtained. The stress intensity factors are

$$k_1 = \frac{1}{2\pi^2\sqrt{|z|}} PG_1(b/|z|)$$

$$k_2 = \frac{1}{2\pi^2\sqrt{|z|}} \{QG_1(b/|z|) + \frac{2\nu}{2-\nu}[QG_2(b/|z|)$$

$$- Rsgn(z)G_3(b/|z|)]\} \qquad (22)$$

$$k_3 = \frac{1}{2\pi^2\sqrt{|z|}} \{RG_1(b/|z|) + \frac{2\nu}{2-\nu}[RG_2(b/|z|)$$

$$- Qsgn(z)G_3(b/|z|)]\}$$

where

$$G_1(\eta) = g_1(\eta) - 2\eta g_1'(\eta) = 2g_2(\eta)$$

$$G_2(\eta) = g_2(\eta) - 2\eta g_2'(\eta) \qquad (23)$$

$$G_3(\eta) = g_3(\eta) - 2\eta g_3'(\eta)$$

Point loads. From either of the two previous special cases the solution for the case of point loads (equations (6) and (7)) can be recovered by holding the total load constant while decreasing the length of the line to zero.

Two-dimensional problems. The length of the line parallel to the z-axis on which loads are applied to produce stress intensity factors given as described prior to equations (21) can be increased indefinitely. It can be verified

that the two-dimensional results

$$k_1 = \frac{P}{\pi}\sqrt{\frac{2}{a}},\quad k_2 = \frac{Q}{\pi}\sqrt{\frac{2}{a}},\quad k_3 = \frac{R}{\pi}\sqrt{\frac{2}{a}} \tag{24}$$

are recovered.

A second two-dimensional result is obtained by letting $a\to\infty$ in equations (10), (11), and (12). This corresponds to uniform stresses on the entire strip $y=0$, $-b<x<0$, $|z|<\infty$ of the surfaces of the crack and gives the stress intensity factors

$$k_1 = \frac{2}{\pi}\, p\sqrt{2b},\quad k_2 = \frac{2}{\pi}\, q\sqrt{2b},\quad k_3 = \frac{2}{\pi}\, r\sqrt{2b} \tag{25}$$

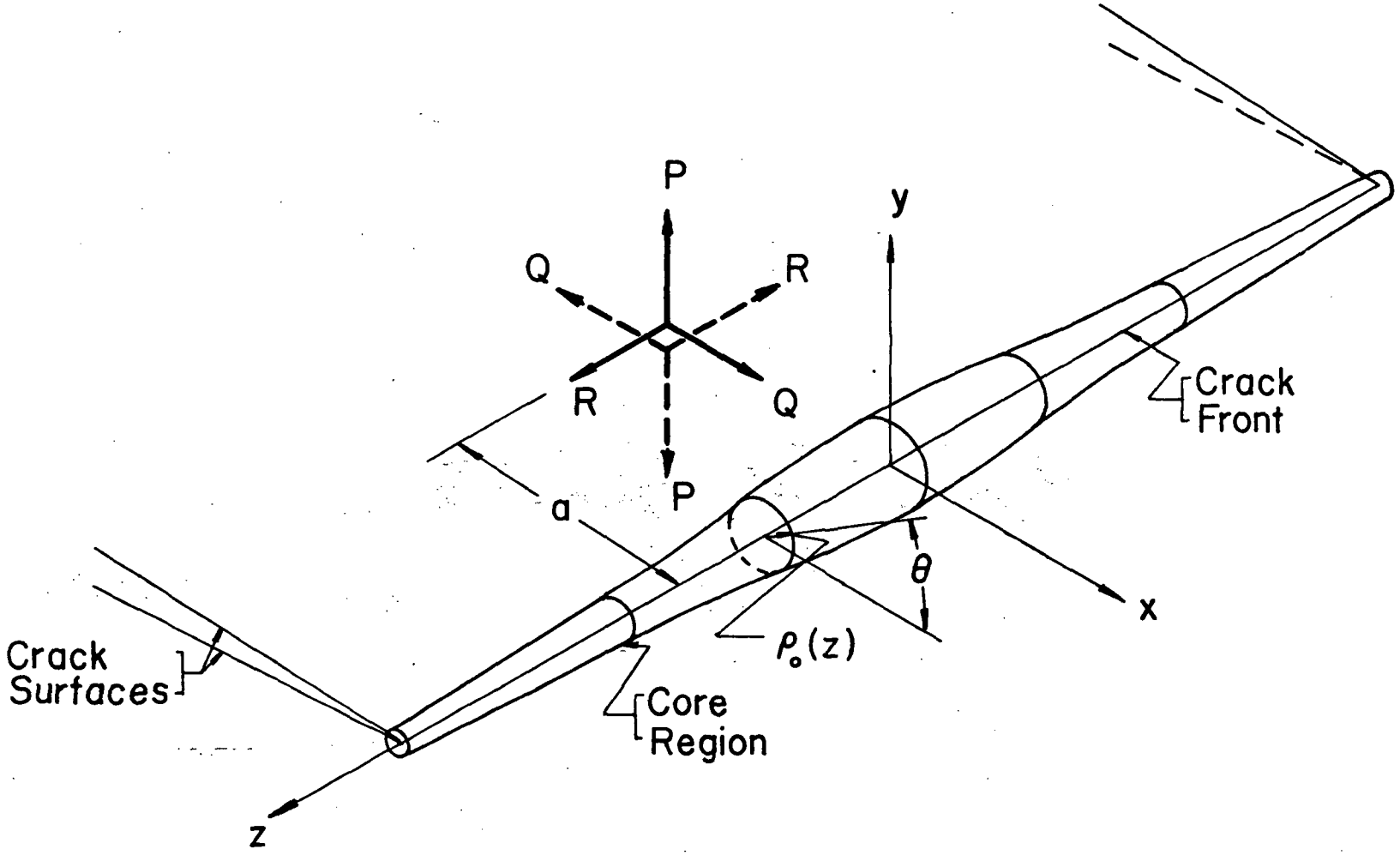


Figure 1: A half plane (y=0, x<0) crack in an infinite body with equal and opposite forces applied to the upper surface at $(-a,0^+,0)$ and to the lower surface at $(-a,0^-,0)$. A core region of variable radius, $\rho_o(z)$, is also shown.

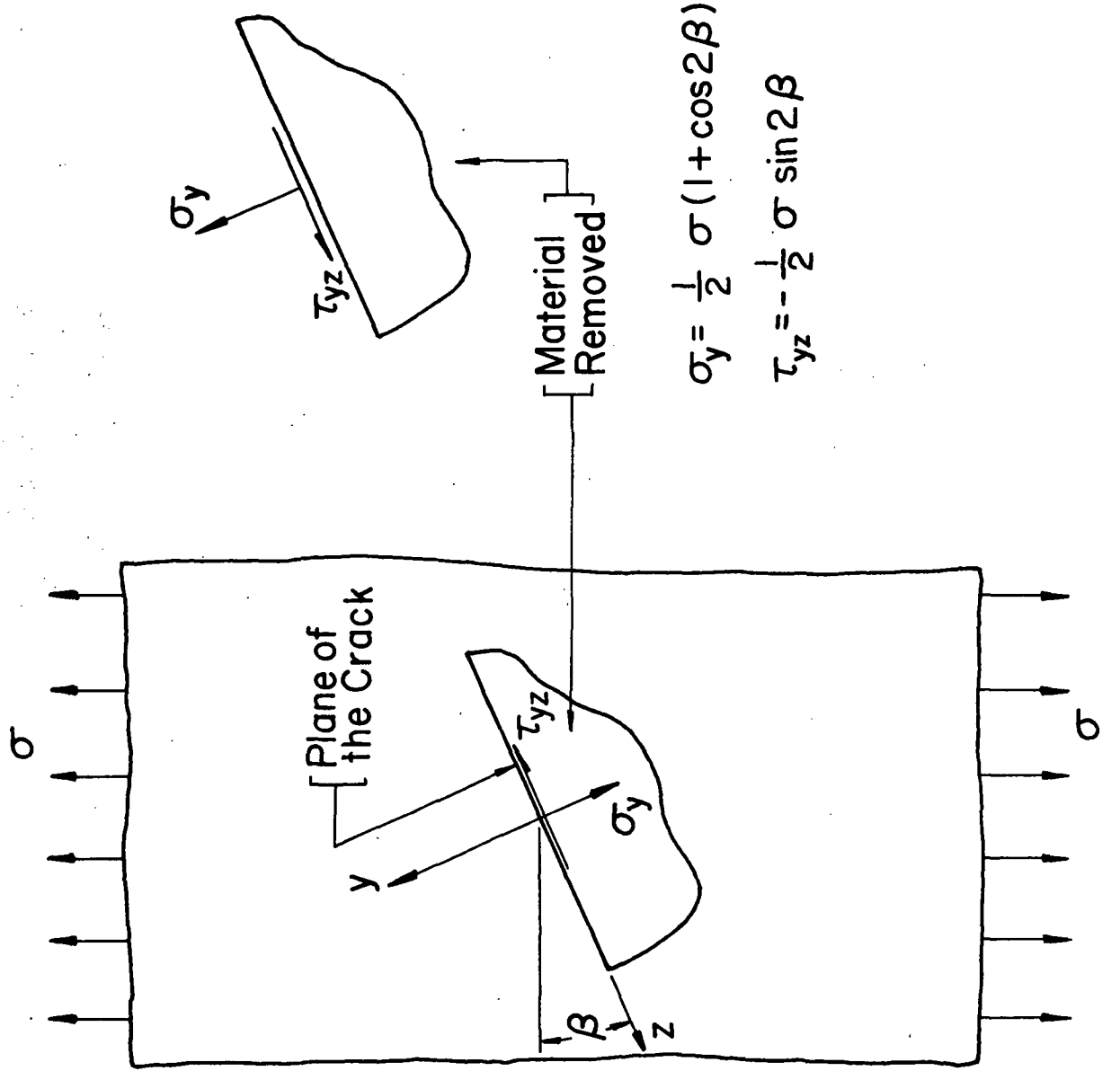


Figure 2: The stresses on an oblique plane in a state of uniform stress.

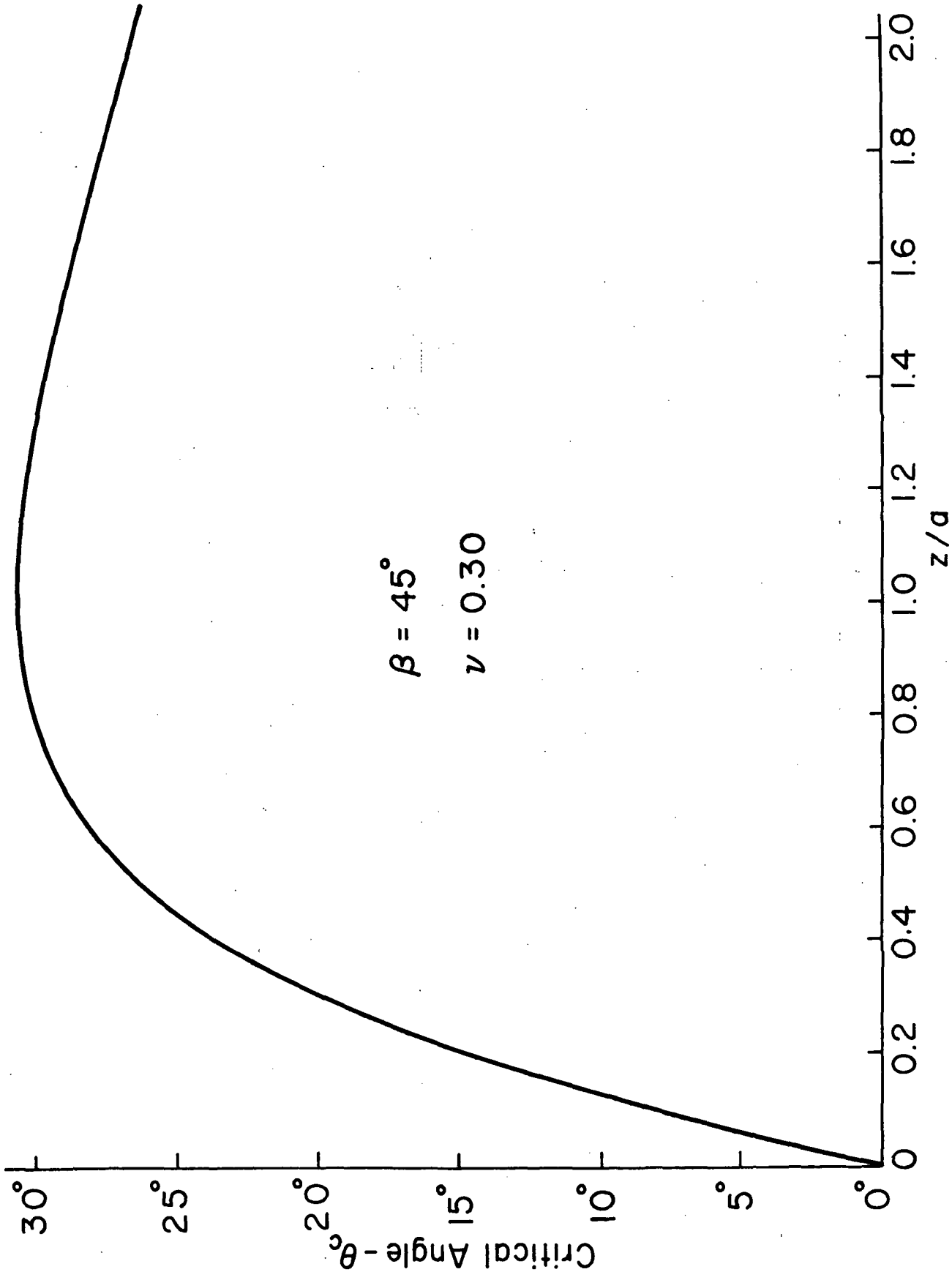


Figure 3: Directions of crack extension as a function of distance along crack front for concentrated forces.

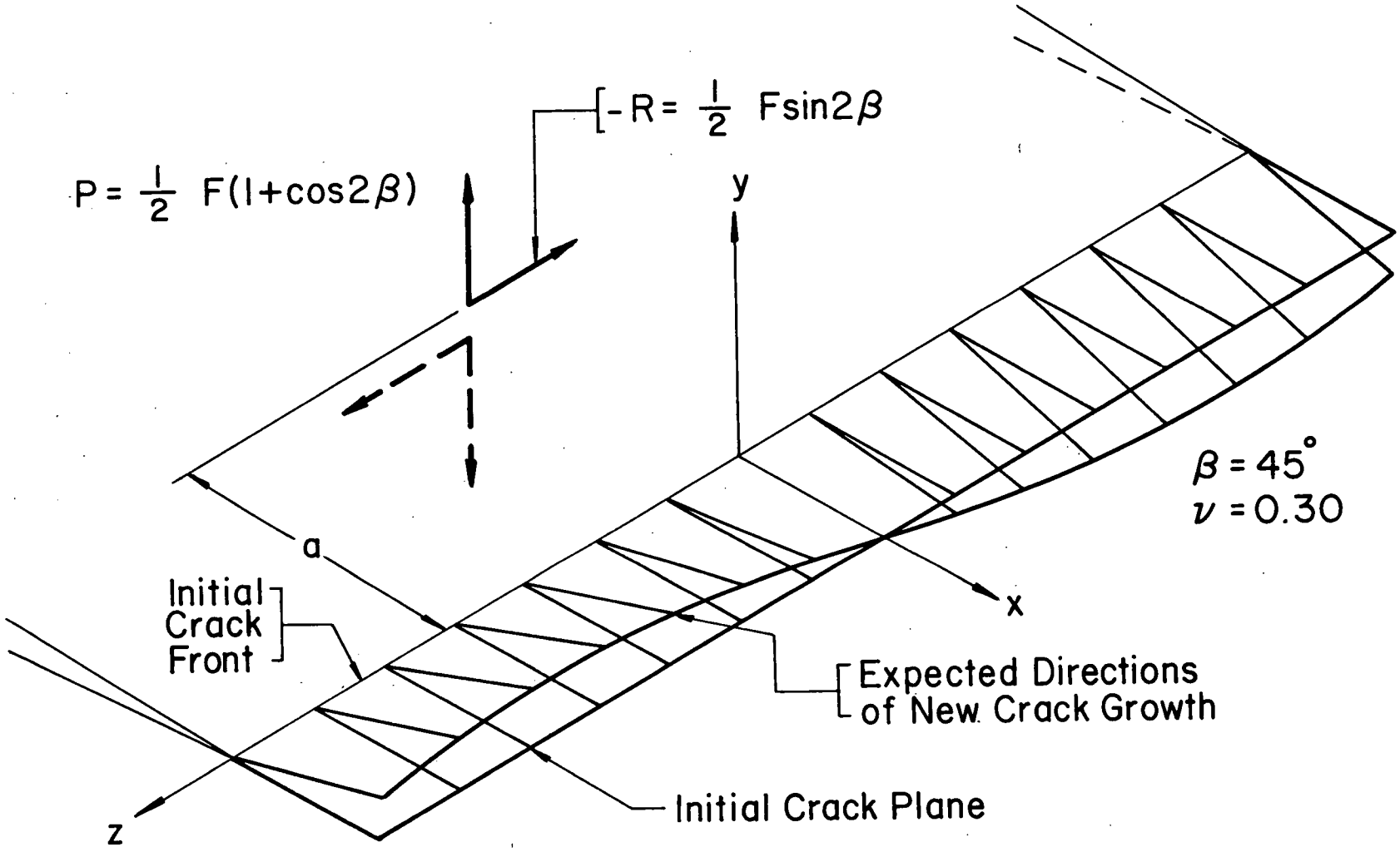


Figure 4: Expected directions of growth of a crack subjected to concentrated forces.

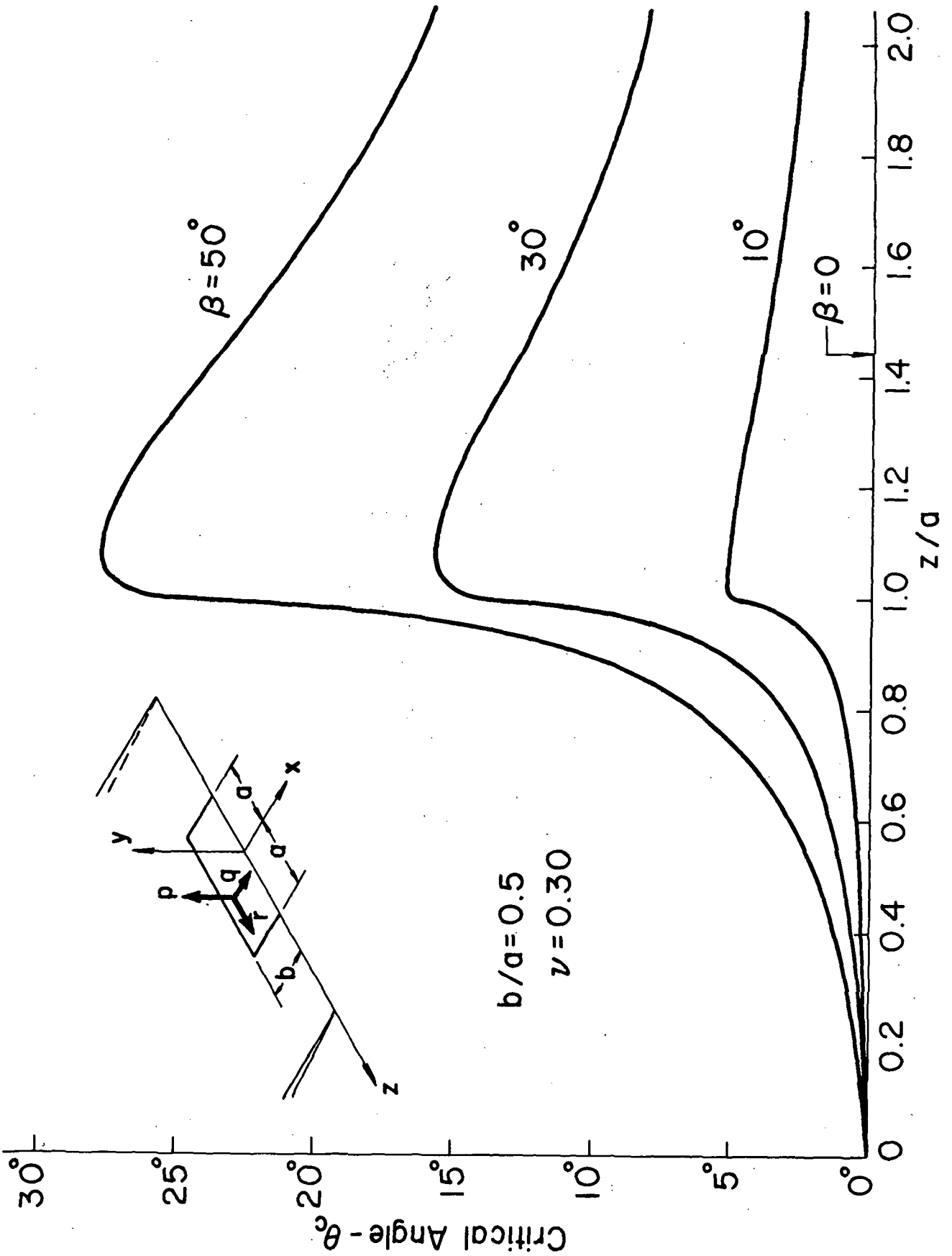


Figure 5: *Directions of crack extension as a function of distance along crack front for uniform stresses applied to a b×2a rectangular portion of the crack surfaces.* b/a = 0.5.

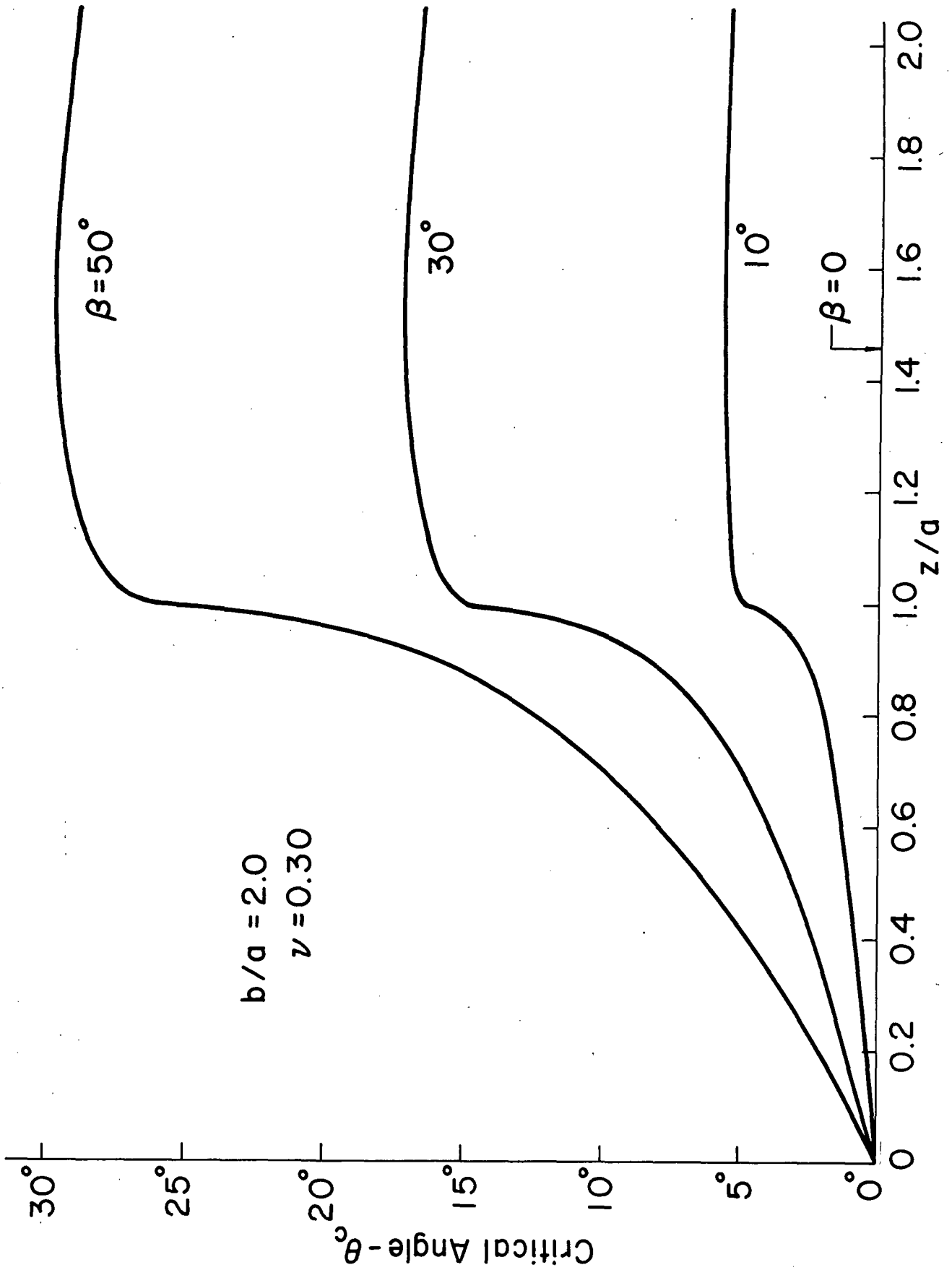


Figure 6: Directions of crack extension as a function of distance along crack front for uniform stresses applied to a b×2a rectangular portion of the crack surfaces. b/a = 2.0.

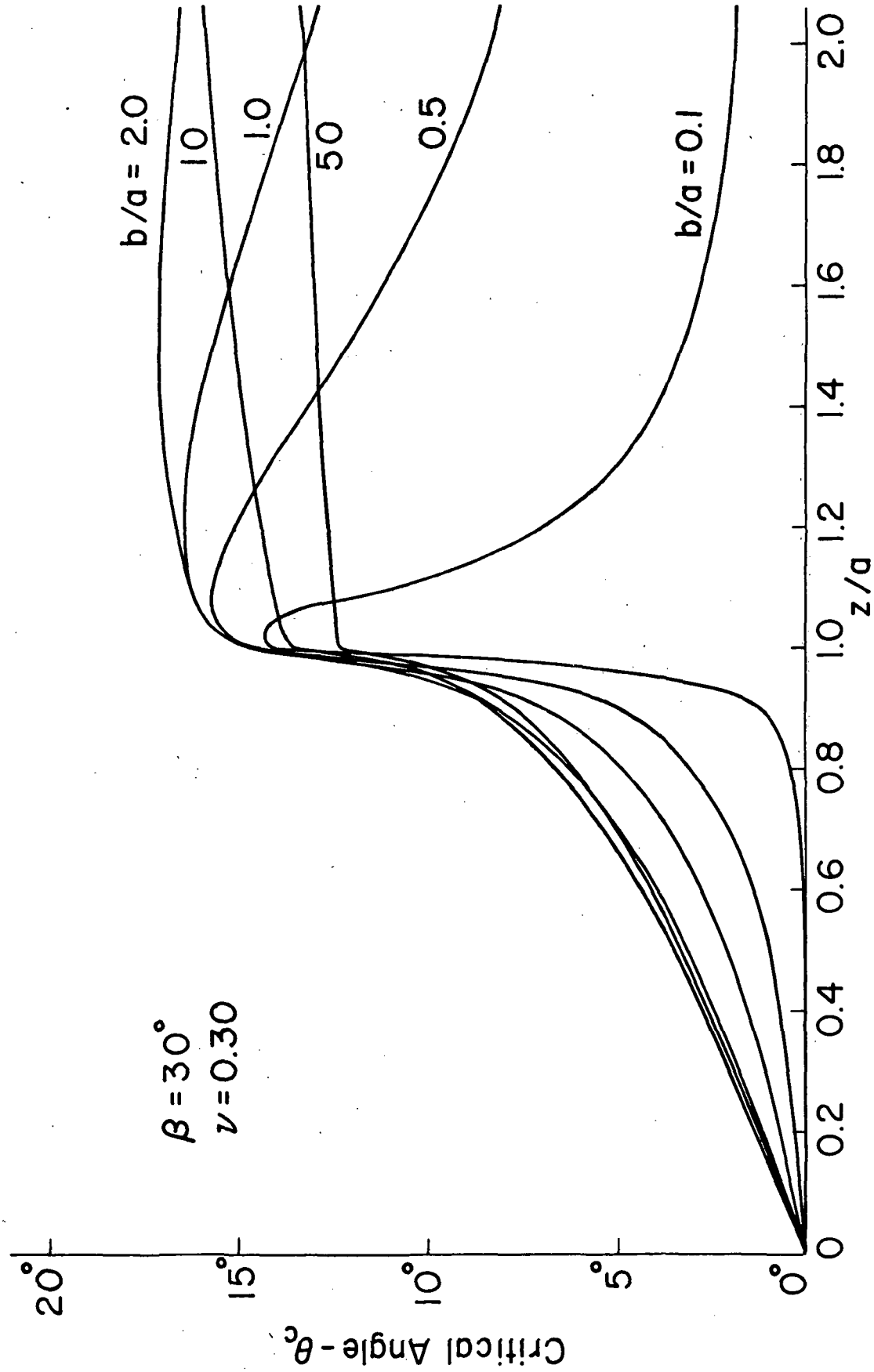


Figure 7: Effect of proportions of uniformly loaded rectangle on the expected directions of crack growth. $\beta = 30°$.

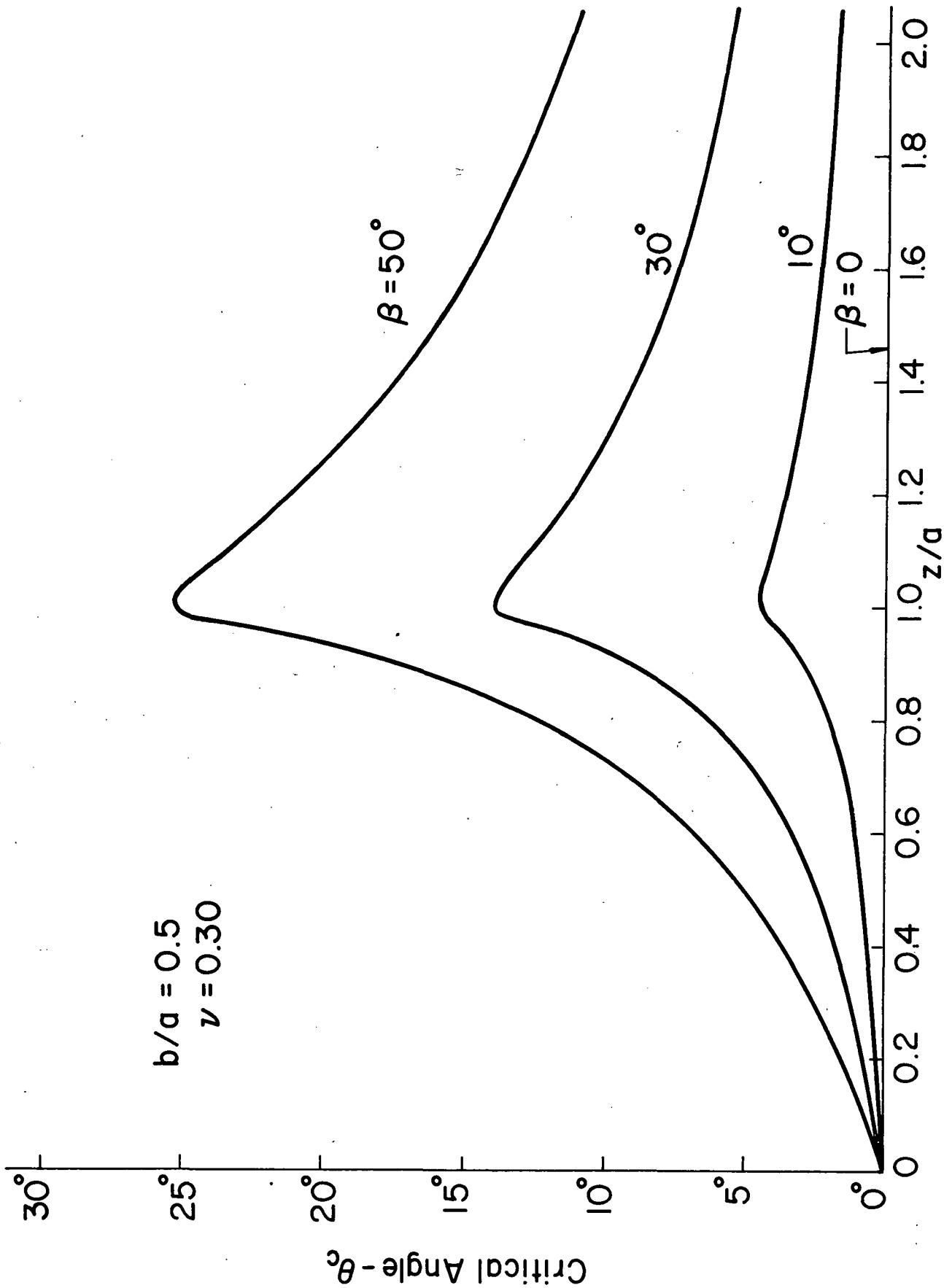


Figure 8: Effect of non-uniform distribution (equation (16)) of stress on a b×2a portion of the crack surfaces on the directions of crack extension. b/a = 0.5.

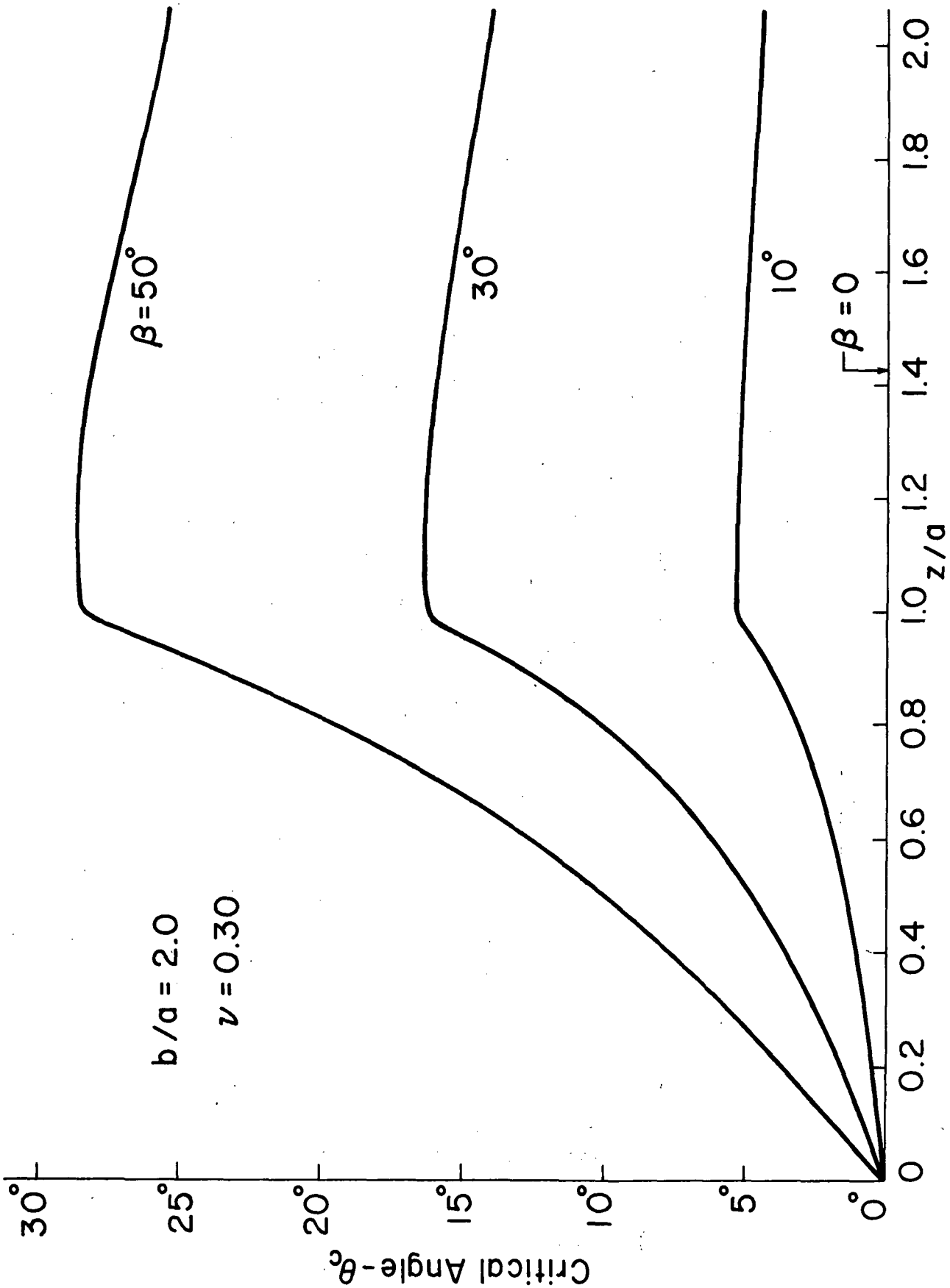


Figure 9: Effect of non-uniform distribution (equation (16)) of stress on a b×2a portion of the crack surfaces on the directions of crack extension. b/a = 2.0.

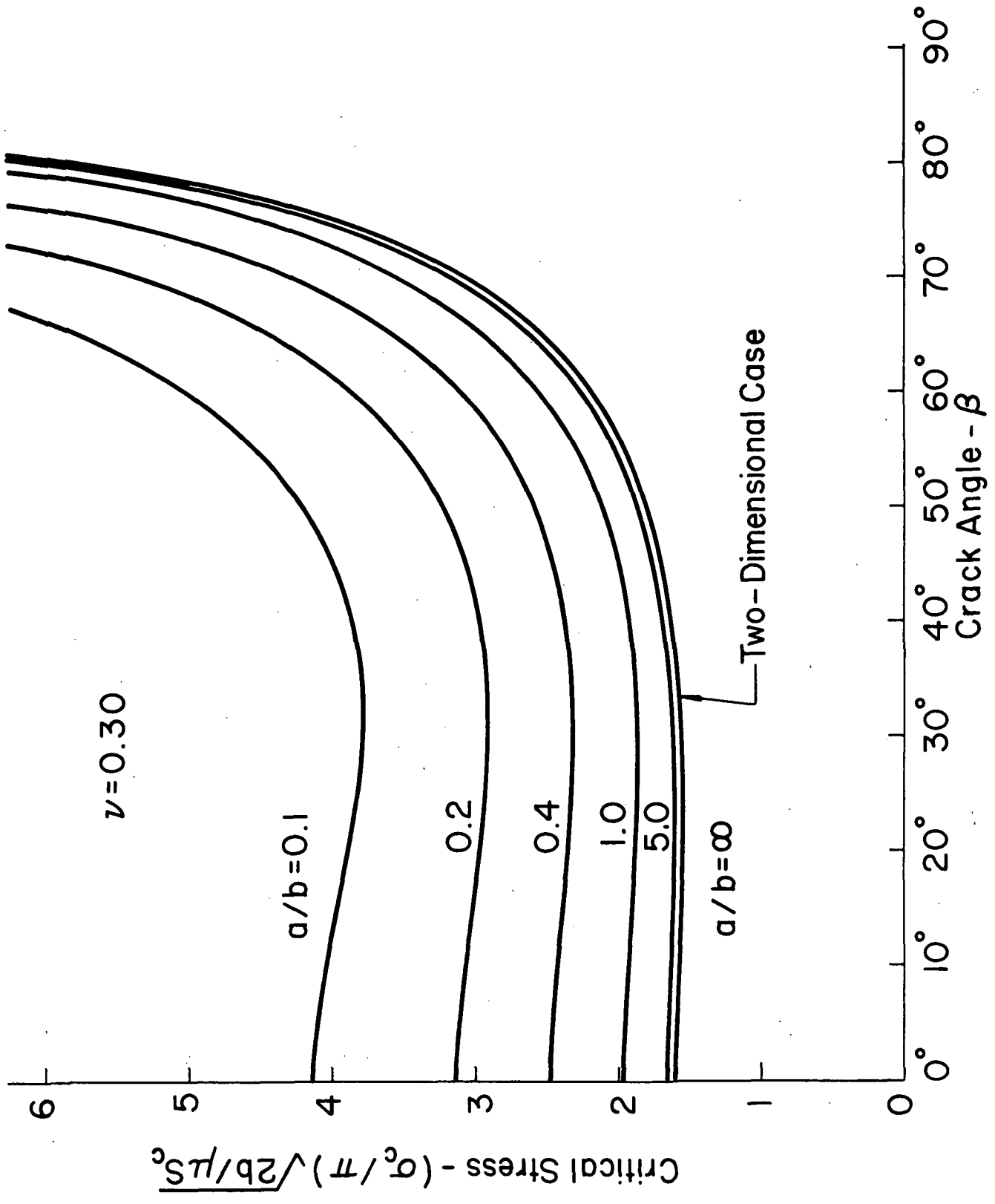


Figure 10: Fracture value of applied stress for the uniform stress case vs. angle of load.

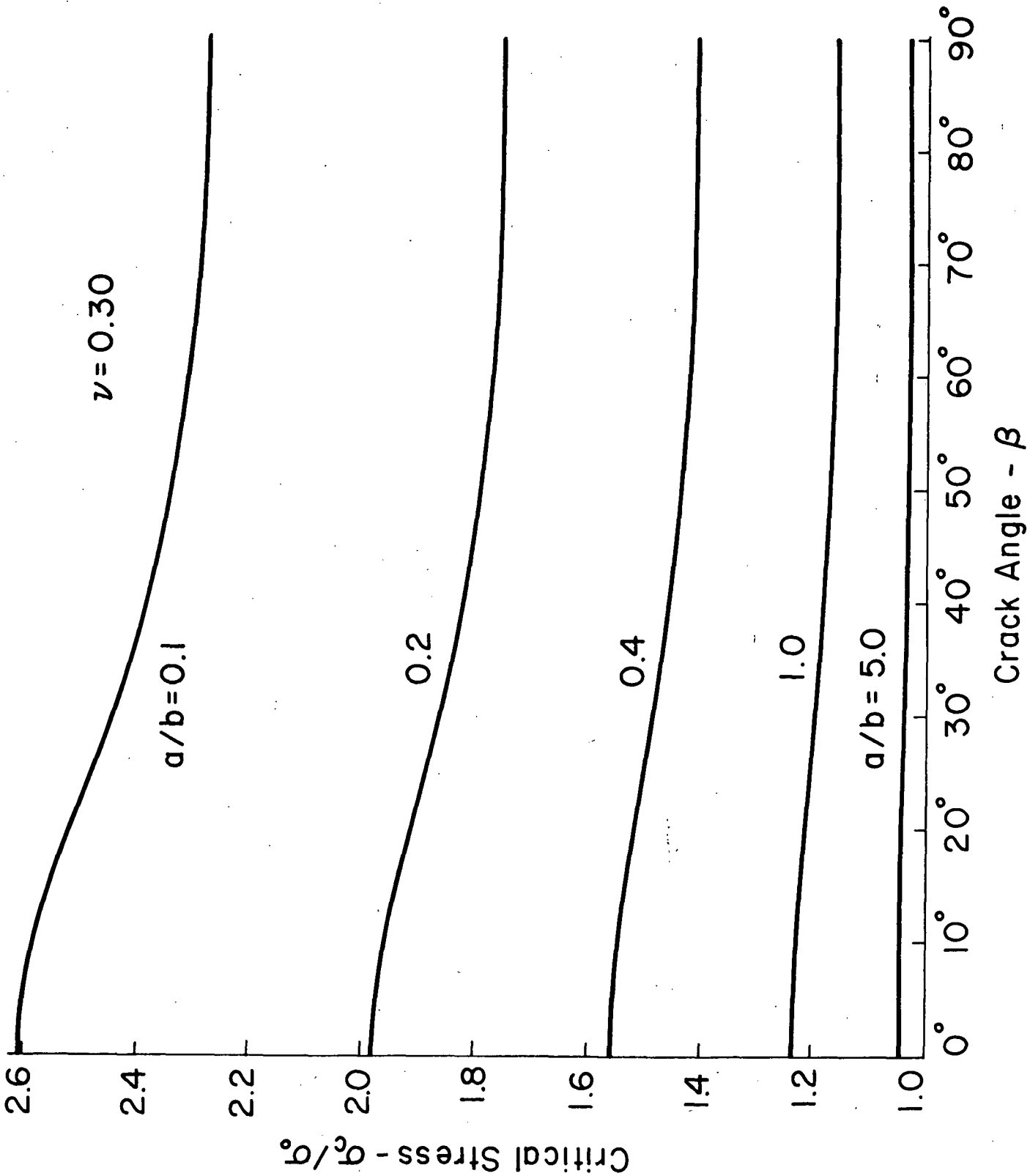


Figure 11: Fracture stress normalized by the two-dimensional value vs. angle of load.

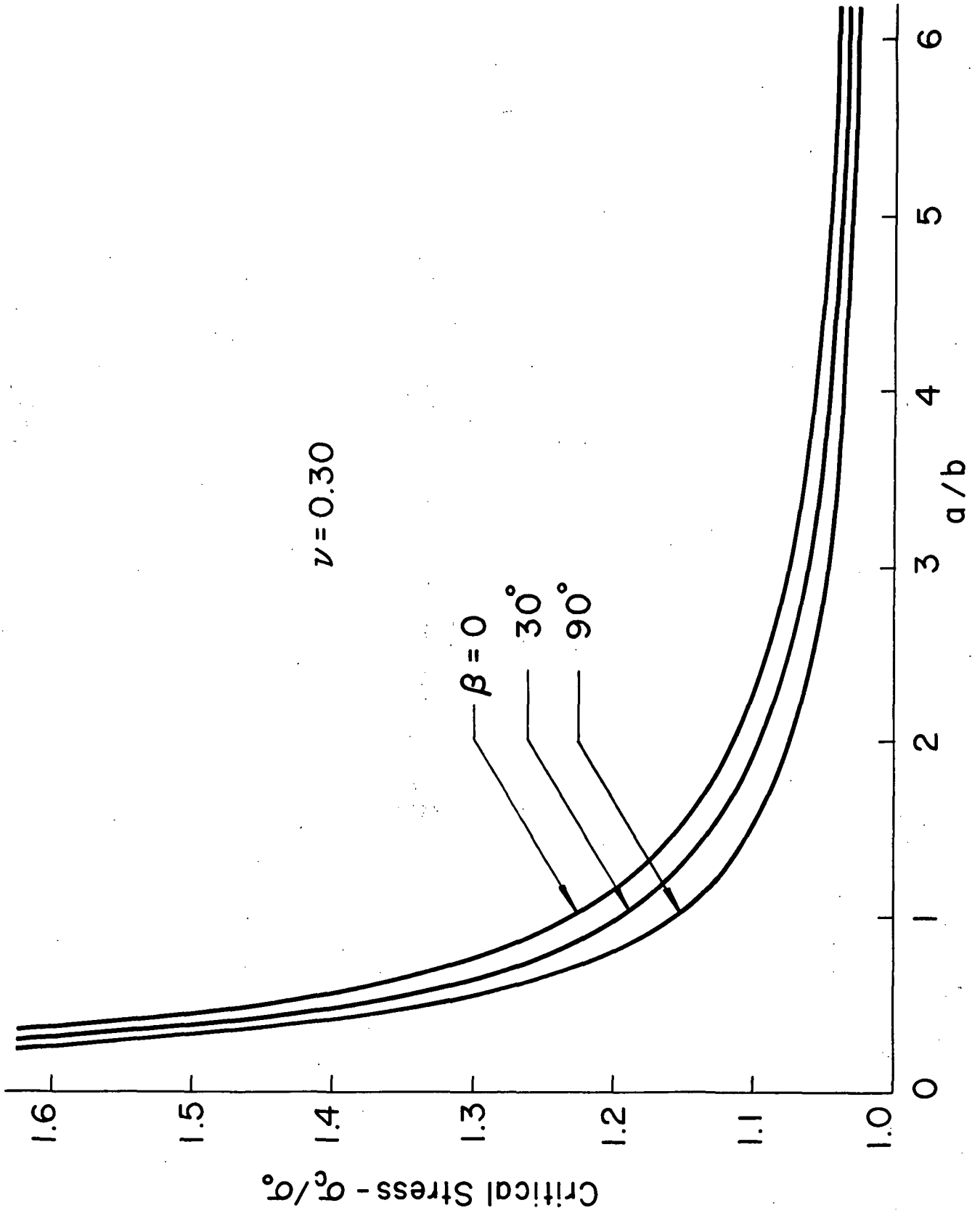


Figure 12: Normalized fracture stress vs. proportions of the rectangular area of application of uniform stresses.